Arg206 of SNAP-25 is essential for neuroexocytosis at the *Drosophila melanogaster* neuromuscular junction

Aram Megighian[1,*], Michele Scorzeto[1,*], Damiano Zanini[1,2,*], Sergio Pantano[3], Michela Rigoni[4], Clara Benna[2], Ornella Rossetto[4], Cesare Montecucco[4,‡] and Mauro Zordan[2]

[1]Department of Human Anatomy and Physiology, Section of Physiology, University of Padova, 35131, Italy
[2]Department of Biology, University of Padova, 35121, Italy
[3]Biomolecular Simulations Group, Institut Pasteur de Montevideo, Mataojo 2020, CP 11400, Montevideo, Uruguay
[4]Department of Biomedical Sciences, University of Padova, 35121, Italy
*These authors contributed equally to this work
‡Author for correspondence (cesare.montecucco@gmail.com)

Accepted 17 June 2010
Journal of Cell Science 123, 3276-3283

doi:10.1242/jcs.071316

Summary

An analysis of SNAP-25 isoform sequences indicates that there is a highly conserved arginine residue (198 in vertebrates, 206 in the genus *Drosophila*) within the C-terminal region, which is cleaved by botulinum neurotoxin A, with consequent blockade of neuroexocytosis. The possibility that it may play an important role in the function of the neuroexocytosis machinery was tested at neuromuscular junctions of *Drosophila melanogaster* larvae expressing SNAP-25 in which Arg206 had been replaced by alanine. Electrophysiological recordings of spontaneous and evoked neurotransmitter release under different conditions as well as testing for the assembly of the SNARE complex indicate that this residue, which is at the P_1' position of the botulinum neurotoxin A cleavage site, plays an essential role in neuroexocytosis. Computer graphic modelling suggests that this arginine residue mediates protein–protein contacts within a rosette of SNARE complexes that assembles to mediate the fusion of synaptic vesicles with the presynaptic plasma membrane.

Key words: *Drosophila melanogaster*, SNAP-25, SNARE, SNARE supercomplex, Synaptic vesicle fusion

Introduction

SNARE proteins are the main molecular constituents of the synaptic vesicle (SV) fusion machinery. A four helix bundle spontaneously forms by coil-coiling of the cytoplasmic domains of the three SNARE proteins: VAMP (also known as synaptobrevin), syntaxin and SNAP-25. The assembly of the SNARE complex is essential for the synaptic vesicle fusion process (Jahn and Scheller, 2006; Sudhof and Rothman, 2009). It has been estimated that the formation of three or more SNARE complexes provides sufficient free energy to drive membrane fusion (Cohen and Melikyan, 2004; Li et al., 2007; Sudhof and Rothman, 2009), but the energetic yield of the process is not known. Additional proteins (rab-GTPases, MUNC and RIM proteins, complexin, syntaxin and others) are involved in regulation binding of the SV to the cytosolic face of the presynaptic membrane and in Ca^{2+}-triggered fusion; the local Ca^{2+} concentration rises following the opening of voltage-gated Ca^{2+} channels located close to the active zones where fusion takes place (Brose, 2008; Rizo and Rosenmund, 2008; Brunger et al., 2009; Ohya et al., 2009; Sudhof and Rothman, 2009). The time delay between the cytosolic Ca^{2+} trigger and the fusion of docked and ready-to-release SVs varies for different synapses, but it is always very short (>100 microseconds) (Kasai, 1999; Zenisek et al., 2000; Sudhof and Malenka, 2008). This very short time period indicates that the ready-to-fuse vesicles may be actually in a state of hemifusion with the presynaptic membrane (Giraudo et al., 2005; Chernomordik and Kozlov, 2008; Lu et al., 2008). This would require that the SVs are actually stably juxtaposed on the cytosolic face of the presynaptic membrane and this appears to involve several SNARE complexes at the same site.

Convincing evidence for the key role of the three neuronal SNARE proteins in neurotransmitter release derives from its complete blockade exerted by tetanus and botulinum neurotoxins (Schiavo et al., 1992; Blasi et al., 1993; Schiavo et al., 1993a; Rossetto et al., 2001). Botulinum neurotoxin type A (BoNT/A) cleaves SNAP-25 nine residues from the C-terminus (Schiavo et al., 1993b; Binz et al., 1994) suggesting that this part of the molecule plays a central role in the assembly and/or function of the neuroexocytosis machinery. We have begun a detailed investigation of this SNAP-25 region by site-directed mutagenesis in *Drosophila melanogaster* coupled to electrophysiological recording of the *Drosophila* larva neuromuscular junction (NMJ). We started with an analysis of the available sequences of neuronal SNAP-25 and related isoforms reported in databases. As expected, mapping of the conservation profiles into the structure of the SNARE complex (Chen et al., 2002) shows a high conservation for residues involved in intermolecular contacts within each SNARE four-helix bundle (Fasshauer et al., 1998; Jahn and Scheller, 2006; Sorensen, 2009). We have, as well, considered external residues which are essential for possible protein–protein contacts that are necessary to form a rosette of SNARE complexes. The formation and involvement of such a rosette in neuroexocytosis is suggested by several findings and considerations (Fasshauer et al., 1998; Hua and Scheller, 2001; Tokumaru et al., 2001; Keller et al., 2004; Montecucco et al., 2005; Rickman et al., 2005; Lu et al., 2008; Sorensen, 2009). There is a single amino acidic residue that is fully conserved among species and isoforms of SNAP-25, not involved in the zippering of the SNARE complex, and this is Arg198 (mouse and human SNAP-25 numbering), which points outside of the four-helix bundle SNARE complex in the C-terminal of SNAP-25. This residue is at

the P_1' site of the peptide bond cleaved by BoNT/A (de Paiva et al., 1993).

On this basis, we hypothesize that site-directed substitution of Arg198 with a neutral residue could interfere, in vivo, with the function of the neuroexocytosis apparatus in such a way as to be detectable by electrophysiological recordings at the neuromuscular junction. To test this possibility, we used *Drosophila melanogaster*, as an animal model. Arg198 of human SNAP-25 corresponds to Arg206 of *D. melanogaster* SNAP-25. We generated transgenic lines of *D. melanogaster* carrying SNAP-25 with an alanine at position 206. The transgene was expressed in a wild-type background and resulted in a significant reduction of both evoked and spontaneous neurotransmitter release at the neuromuscular junction in third instar larvae, relative to that in controls, in the absence of overt NMJ morphological defects. This finding is discussed and interpreted in terms of a rosette model for the apparatus that mediates fusion of synaptic vesicles with the presynaptic membrane.

Results

Expression of the SNAP-25^{R206A} mutant in the nervous system of *D. melanogaster*

The expression of SNAP-25^{R206A} using the nervous system driver *ElavGAL4*, is illustrated in Fig. 1A, which shows a representative semiquantitative PCR performed on third instar larval brain. In Fig. 1B, average (± s.d.) relative percentage expression levels of SNAP-25 isoforms (WT or R206A), relative to constitutive SNAP-25 expression in control w^{1118} larval brains are reported. The relative percentage expression of the SNAP-25^{WT} isoform was 136.00±17.28 in *ElavGAL4/UAS–SNAP-25^{WT}* and 106.0±26.3 in *ElavGAL4/UAS–SNAP-25^{R206A}*, whereas for the SNAP-25^{R206A} isoform it was 4.8±3.6 in *ElavGAL4/UAS–SNAP25^{WT}* and 256.0±113.3 in *ElavGAL4/UAS–SNAP-25^{R206A}* larval brains (n=4 for each line and for the control w^{1118} line). On average, SNAP25R^{206A} transgene expression, in a WT background, was 2.5 times the expression of SNAP^{WT} in larval brains.

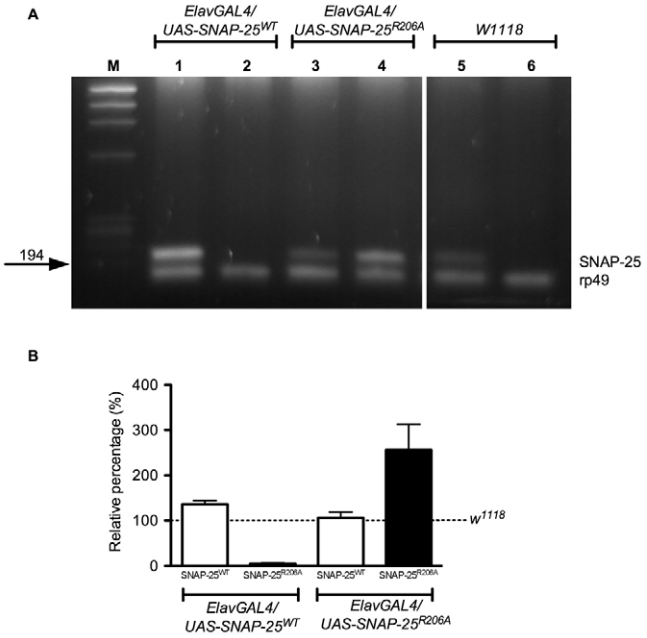

Fig. 1. Semi-quantitative PCR analysis of wild-type (WT) and mutant (R206A) SNAP-25 isoforms in third instar larvae brains. (**A**) Agarose gel electrophoresis of PCR-amplified fragments produced on cDNA from brain total RNA. Lane M is molecular mass markers (*FX174/Hae*III). The bottom-most band in lanes 1–6 is the housekeeping gene *rp49* (164 bp); the other bands are SNAP-25 fragments (WT in lanes 1, 3 and 5; R206A in lanes 2, 4 and 6; 210 bp). (**B**) Average (± s.d.) relative percentage expression levels of SNAP-25 isoforms (WT or R206A) in *ElavGAL4/UAS–SNAP-25^{WT}* (only WT isoform) and *ElavGAL4/UAS–SNAP-25^{R206A}* (WT and R206A isoforms) larval brains (n=4 for each line), relative to constitutive SNAP-25 (=100%; dotted line) expression in control w^{1118} larval brains (n=4).

The presence of SNAP-25^{R206A} at the *D. melanogaster* neuromuscular junction causes a reduction in spontaneous neurotransmitter release

Fig. 2A and Fig. 3A show that the coexpression of SNAP-25^{R206A} with SNAP-25^{WT} leads to a significant (P<0.05) reduction in spontaneous neurotransmitter release. The mean (± s.e.m.) frequency values of spontaneous release were: 1.85±0.35 Hz in *ElavGAL4/UAS–SNAP-25^{WT}* and 1.01±0.11 Hz in *ElavGAL4/UAS–SNAP-25^{R206A}* under current-clamp conditions; under voltage-clamp conditions, these values were: 1.61±0.05 Hz in *ElavGAL4/UAS–SNAP-25^{WT}* and 1.07±0.04 Hz in *ElavGAL4/UAS–SNAP-25^{R206A}*.

The average miniature end-plate potential (MEPP) amplitudes (in current-clamp conditions) were: 0.97±0.06 mV and 0.94±0.02

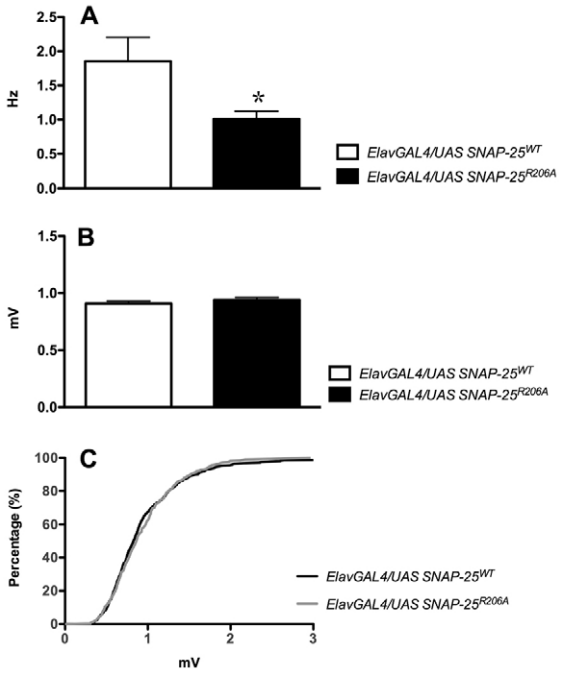

Fig. 2. Spontaneous neurotransmitter release in SNAP-25^{WT} and SNAP-25^{R206A} transgenic third instar larvae, recorded in current-clamp conditions. (**A**) Mean MEPP (± s.e.m.) frequency in *ElavGAL4/UAS–SNAP-25^{WT}* (n=5) and *ElavGAL4/UAS–SNAP-25^{R206A}* (n=5) larvae. As indicated in the text, one neuromuscular junction for each animal was analysed. *Data are statistically different (P<0.05; Student's t-test for unpaired data). (**B**) Mean (± s.e.m.) MEPP amplitude in *ElavGAL4/UAS–SNAP-25^{WT}* (556 events analysed from five different larvae) and *ElavGAL4/UAS–SNAP-25^{R206A}* (314 events analysed in five different larvae). Data are not statistically significantly different (Student's t-test for unpaired data). (**C**) Relative cumulative frequency distribution of MEPP amplitudes from *ElavGAL4/UAS–SNAP-25^{WT}* (black line) and *ElavGAL4/UAS–SNAP-25^{R206A}* (grey line). Data are not statistically different (Kolmogorov–Smirnov test; see Results section).

mV in *ElavGAL4/UAS–SNAP-25^{WT}* and *ElavGAL4/UAS–SNAP-25^{R206A}*, respectively (Fig. 2B). Data were not significantly different (Student's *t*-test for unpaired samples). Fig. 2C shows that the cumulative MEPP amplitudes distributions were not significantly different (Kolmogorov–Smirnov *D*=0.069; *P*=NS).

By contrast, the average miniature end plate current (MEPC) amplitude (under voltage-clamp conditions) was significantly reduced in *ElavGAL4/UAS–SNAP-25^{R206A}* (132.6±2.2 pA; mean ± s.e.m.) with respect to *ElavGAL4/UAS–SNAP-25^{WT}* (167.8±2.5 pA; mean ± s.e.m.; Fig. 3B). And this is reflected in the cumulative MEPC amplitudes distributions, showing a shift towards smaller amplitudes in the case of *ElavGAL4/UAS–SNAP-25^{R206A}* (Kolmogorov–Smirnov *D*=0.186; *P*=0.001; Fig. 3C).

Spontaneous fusions occur in a random manner, each event being independent from the previous and next one. Accordingly, the frequency distribution of MEPCs inter-event intervals is well described by a Poisson distribution in both controls and SNAP-25^{R206A} mutants (Fig. 3D), indicating that the random nature of spontaneous fusion was not altered by the presence of SNAP-25^{R206A}.

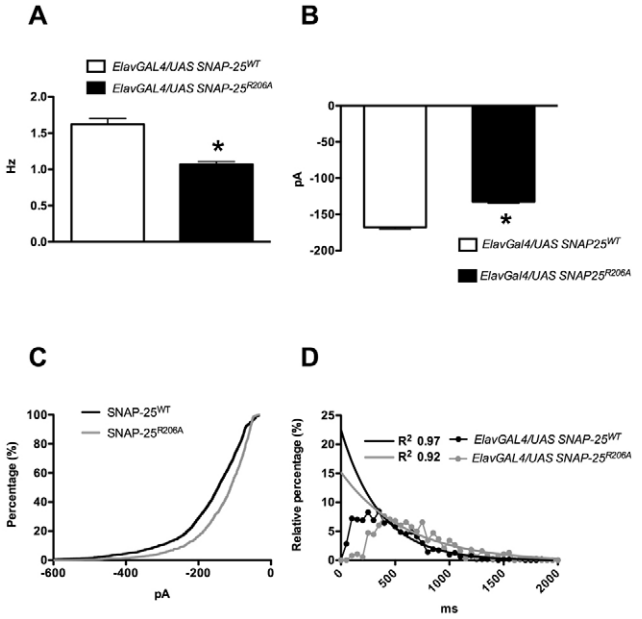

Fig. 3. Spontaneous neurotransmitter release in SNAP-25^{WT} and SNAP-25^{R206A} transgenic third instar larvae, recorded in voltage-clamp conditions. (**A**) Mean MEPC (± s.e.m.) frequency in *ElavGAL4/UAS–SNAP-25^{WT}* (*n*=7) and *ElavGAL4/UAS–SNAP-25^{R206A}* (*n*=6) larvae; *n* indicates the number of neuromuscular junctions analysed. One neuromuscular junction for each animal was analysed. *Data are statistically different (*P*<0.05; Student's *t*-test for unpaired data). (**B**) Mean (± s.e.m.) MEPC amplitude in *ElavGAL4/UAS–SNAP-25^{WT}* (2616 events analysed in seven different NMJs) and *ElavGAL4/UAS–SNAP-25^{R206A}* (1539 events analysed in six different NMJs). *Data are statistically different (*P*<0.05; Student's *t*-test for unpaired data). (**C**) Relative cumulative frequency distribution of MEPC amplitudes from *ElavGAL4/UAS–SNAP-25^{WT}* (black line) and *ElavGAL4/UAS–SNAP-25^{R206A}* (grey line). Data are statistically different (Kolmogorov–Smirnov test; see Results section). (**D**) Percentage relative frequency distribution of inter-event intervals (black dots: *ElavGAL4/UAS–SNAP-25^{WT}*; grey dots: *ElavGAL4/UAS–SNAP-25^{R206A}*). Black and grey lines are the monoexponential curve fitting of *ElavGAL4/UAS–SNAP-25^{WT}* and *ElavGAL4/UAS–SNAP-25^{R206A}*data, respectively. The good R^2 (see values in the graph) of each curve fit indicates the random behaviour of spontaneous neurotransmitter release.

The presence of SNAP-25^{R206A} at the *D. melanogaster* neuromuscular junction causes a reduction of evoked end plate potential

Fig. 4 shows that the mean amplitude of evoked junction potentials (EJPs) recorded at third instar larva NMJ following segmental nerve stimulation, was clearly (*P*<0.05) reduced in SNAP-25^{R206A} mutants, with respect to the controls (33.67±0.62 mV in *ElavGAL4/UAS–SNAP-25^{WT}* and 26.04±0.28 mV in *ElavGAL4/UAS–SNAP-25^{R206A}*; mean ± s.e.m.; *n*=6 and 11, respectively).

The presence of SNAP-25^{R206A} at the *D. melanogaster* neuromuscular junction does not alter the Ca^{2+} dependency of neuroexocytosis or the time course of formation of the SNARE complex

SNAP-25 is involved in the control of Ca^{2+} dynamics (close to) at the active zone (Pozzi et al., 2008) and interacts with the voltage-gated Ca^{2+} channel via its C-terminus (Catterall, 1999; Zhong et al., 1999). Indeed, it has been well documented that high external Ca^{2+} concentrations can partially rescue the neuroexocytosis-blocking effect of botulinum neurotoxin type A which cleaves SNAP-25 at the Gln198–Arg199 peptide bond (Schiavo et al., 1993b; Binz et al., 1994). To test for the possibility that the Arg–Ala replacement affects the Ca^{2+} sensitivity of neuroexocytosis, the Ca^{2+} dependence of evoked neurotransmitter release was measured. We observed a reduced Ca^{2+} sensitivity in SNAP-25^{R206A} compared with SNAP-25^{WT} (Fig. 5A) with no change in the slope of the linear fit to the data of voltage change recorded at different

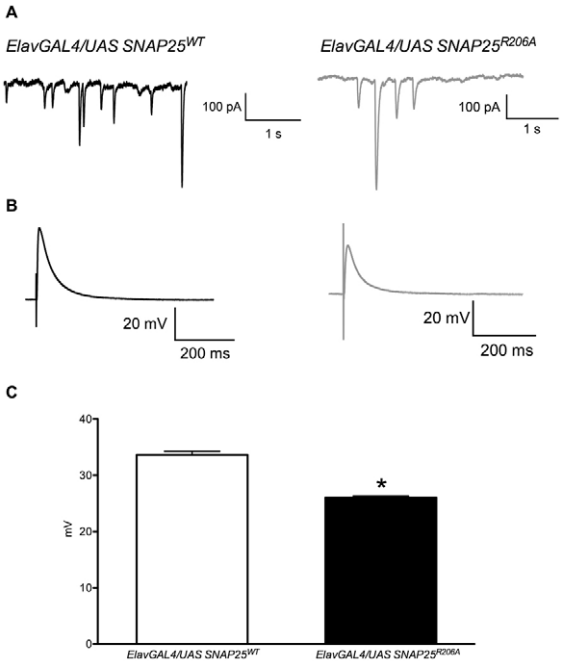

Fig. 4. Evoked neurotransmitter release. (**A**) Representative traces of MEPCs recorded in individual *ElavGAL4/UAS–SNAP-25^{WT}* (black line) and *ElavGAL4/UAS–SNAP-25^{R206A}* (grey line) larvae. (**B**) Representative traces of EJPs recorded in individual *ElavGAL4/UAS–SNAP-25^{WT}* (black line) and *ElavGAL4/UAS–SNAP-25^{R206A}* (grey line) larvae. (**C**) Mean ± s.e.m. amplitude of EJPs in fibre 6 or 7 NMJ by stimulation of the nerve of abdominal segmental 3 in *ElavGAL4/UAS–SNAP-25^{WT}* (*n*=6) and *ElavGAL4/UAS–SNAP-25^{R206A}* (*n*=11) third instar larvae. Extracellular Ca^{2+} concentration was 1 mM. *P<0.05; Student's *t*-test for unpaired data.

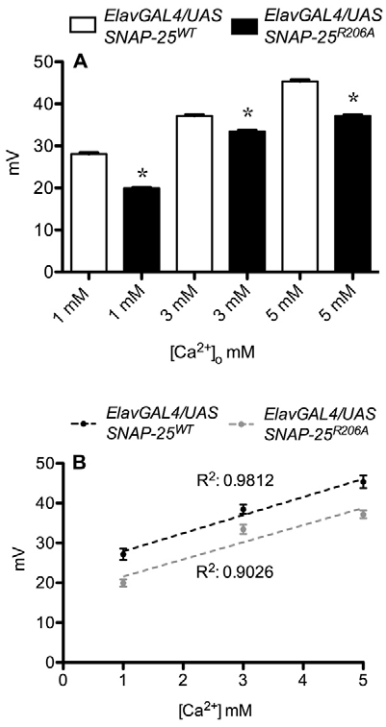

Fig. 5. Calcium sensitivity of evoked release. (**A**) Mean ± s.e.m. amplitude of EJPs evoked in fibre 6 or 7 NMJ by stimulation of the nerve of abdominal segment 3 or 4 fibre at different extracellular Ca^{2+} concentrations in *ElavGAL4/UAS–SNAP-25^{WT}* (*n*=8; white bars) and *ElavGAL4/UAS–SNAP-25^{R206A}* (*n*=9; black bars) third instar larvae. Only fibres in which it was possible to maintain the intracellular recording throughout the whole experiments (i.e. at different external Ca^{2+} concentrations) were considered for analysis. *Statistically significant (P<0.05) difference at each Ca^{2+} concentration tested (Student's *t*-test for unpaired data). (**B**) Linear regression of the same data as in A. R^2 for each linear regression is indicated for the wild-type SNAP-25 (black) and mutated SNAP-25 (grey) samples.

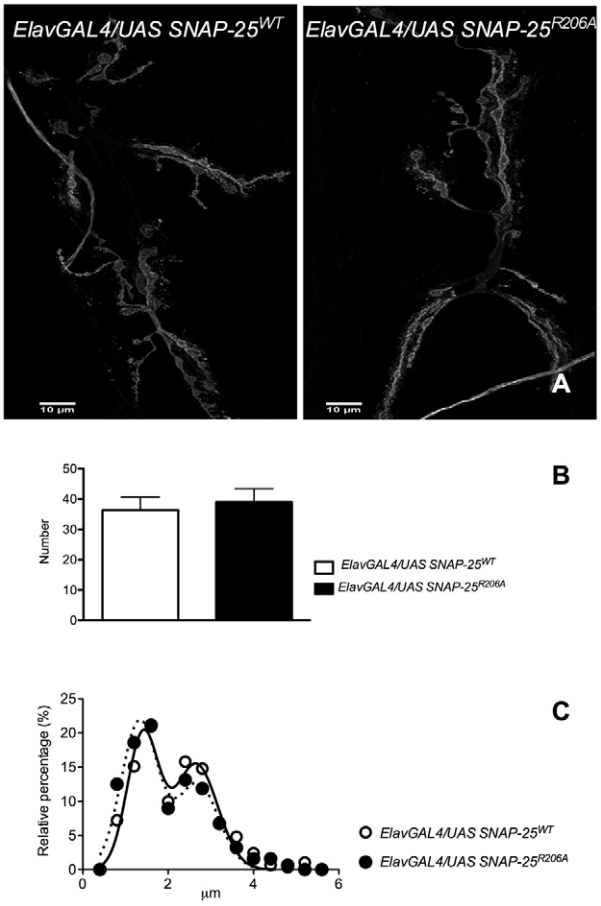

Fig. 6. Third instar larvae NMJ morphological and morphometrical analyses. (**A**) Immunohistochemical staining of abdominal segment 3 fibres 6 and 7 NMJ with the neuronal membrane marker Rhodamine-conjugated anti-HRP antibody. (**B**) Mean (± s.e.m.) number of NMJ type 1b and 1s boutons from abdominal segment 3 fibre 6/7 of *ElavGAL4/UAS–SNAP-25^{WT}* (*n*=8) and *ElavGAL4/UAS–SNAP-25^{R206A}* (*n*=8). (**C**) Relative percentage frequency distribution of type 1b and 1s bouton diameters. Data were fitted with a double Gaussian function (R^2=0.95 and 0.94 for *ElavGAL4/UAS–SNAP-25^{WT}* and *ElavGAL4/UAS–SNAP-25^{R206A}* data, respectively) showing the presence of a double peak corresponding to type 1b and type 1s bouton diameters.

extracellular Ca^{2+} concentrations (Fig. 5B). This result suggests that the Ca^{2+} cooperativity of the process is unchanged between SNAP-25^{R206A} and SNAP-25^{WT} transgenic lines.

The probability of fusion of a synaptic vesicle is strictly dependent on the correct formation of SNARE complexes (Sudhof and Rothman, 2009; Sorensen, 2009) and the results obtained here could reflect defective SNARE complex assembly. We therefore assayed the extent and time-course of the formation of SNARE complexes using GST–SNAP-25^{WT} or the mutant GST–SNAP-25^{R198A} and the cytoplasmic domains of VAMP and syntaxin using established methods (Fasshauer et al., 1998; Fasshauer et al., 2002; Hu et al., 2002). Supplementary material Fig. S1A shows that no difference in the formation of the SNARE complex in vitro was detected between the wild-type and mutated proteins. Measuring the time-course of the SNARE complex formation is a more sensitive and relevant assay. Supplementary material Fig. S1B shows that both wild-type and mutated SNAP-25 very rapidly formed a SNARE complex with VAMP and syntaxin as found previously (Fasshauer et al., 2002) with no difference in the time course. This is a necessary control, the result of which was almost expected as the mutated residue points outward in the crystallographic structure of the SNARE complex (Sutton et al., 1998; Brunger et al., 2009) and C-terminal mutations of SNAP-25 have been shown not to affect SNARE assembly (Sorensen et al., 2006).

The presence of SNAP-25^{R206A} does not alter morphology and morphometry of the *D. melanogaster* neuromuscular junction

As other *Drosophila* synaptic mutants with alteration in synaptic function were reported to show a morphological change at the level of the NMJ (Budnik and Ruiz-Canada, 2006), we analysed the morphology and morphometry of the NMJ after staining with the neuronal-membrane-specific anti-HRP antibody. Fig. 6A shows representative images of the NMJ of muscles 6 and 7 in the abdominal segment A3 of both SNAP-25^{WT} and SNAP-25^{R206A} larvae. Morphometrical analysis indicates that neither the total number of boutons per NMJ (Fig. 6B) nor the diameter of type 1b and 1s boutons were changed in SNAP-25^{R206A} compared with SNAP-25^{WT} (Fig. 6C). We did not extend this analysis to the electron microscopic level because the removal from SNAP-25 of

the C-terminal segment beginning with Arg198 by BoNT/A has been previously shown not to change the appearance of the synaptic terminal at this level (Neale et al., 1999).

Discussion

The present finding that the replacement of the conserved Arg198 residue of SNAP-25 with alanine affects the probability of neurotransmitter release is very relevant because it identifies a key residue in this process of paramount importance for the function of the nervous system. However, as the process is a complex one, the end result is open to different interpretations. We provided evidence against the possibilities that: (1) this change might have affected the assembly of the SNARE complex; (2) the calcium concentration dependence of the phenomenon could have been altered; (3) the morphology and/or morphometry of the NMJ was changed. This residue is not involved in the protein–protein interactions between the three SNARE proteins, and points outward, suggesting that it may be involved in the interaction with other proteins of the neuroexocytosis machinery. There are several scattered pieces of evidence that a number of SNARE complexes are involved in the exocytosis of vesicles and granules. Multimers containing a variable number of SNARE complexes have been observed under various circumstances in vitro (Fasshauer et al., 1998; Antonin et al., 2000) and were isolated from detergent-treated squid synaptosomes (Tokumaru et al., 2001). The Ca^{2+}-cooperativity of neurotransmitter release was found to be linked to the number of SNARE proteins (Stewart et al., 2000). Remarkably, star-shaped oligomers, comprising three to four SNARE complexes, were isolated from detergent-treated homogenized bovine brain with a monoclonal antibody directed toward the acetylated N-terminus of SNAP-25 (Rickman et al., 2005). In vitro experiments performed with different biophysical approaches indicate the formation of oligomers of three to ten SNARE complexes (Karatekin et al., 2010; Yersin et al., 2003; Lu et al., 2008).

Using a peptide that inhibits granule fusion in a chromaffin cell line, Hua and Scheller (Hua and Scheller, 2001) estimated that a minimum of three SNARE complexes is sufficient to support exocytosis. In the same PC12 cells, mutagenesis of the trans-membrane domain of the SNARE presynaptic membrane protein syntaxin led to an estimate of five to eight syntaxin molecules being involved in catecholamine release (Han et al., 2004). However, careful experiments performed with mouse spinal cord motoneurons and with the frog NMJ intoxicated with botulinum neurotoxins suggested a higher figure (Raciborska et al., 1998; Keller and Neale, 2001; Keller et al., 2004; Montecucco et al., 2005). The involvement of multi SNARE complexes in neuroexocytosis also accounts for the strikingly long duration of BoNT/A poisoning (>3 months in human skeletal muscles) (Eleopra et al., 1998; Meunier et al., 2003) and for the fact that transfection of BoNT/A-truncated SNAP-25 inhibits exocytosis (Huang et al., 1998; Wei et al., 2000; Fang et al., 2008) [for a discussion see Montecucco et al. (Montecucco et al., 2005)]. On the basis of this rich set of data indicating the role of an oligomeric SNARE super-complex in exocytosis, we have modelled here a ten-SNARE-complex rosette and have run molecular dynamics simulations (Fig. 7). Such modelling is justified by the fact that the three SNARE proteins are sufficient to promote membrane fusion in vitro and can, therefore provide relevant information on protein–protein contacts among SNARE complexes in membranes (Sudhof and Rothman, 2009; Karatekin et al., 2010). Given the necessity of forming a ring of 'petals' to define a central area where membrane fusion may take place, such an approach shows that few protein–protein contacts between SNARE complexes are involved, and Arg198 is at the centre of the contact areas between the petals of the rosette. Changing the number of petals of the rosette between eight and 13 results in little alteration in the amount of protein–protein contacts between each SNARE complex, while Arg198 remains in a central position within the area of contact. The simple replacement of this charged residue with a helix-promoting, but uncharged, alanine residue does not appear to change the secondary structure, and indeed we did not find any effect of the alanine replacement in the rate and extent of assembly of the SNARE complex in vitro (supplementary material Fig. S1). However, this single mutated SNAP-25 is sufficient to decrease the number of miniature end plate potential events as well as evoked end plate potentials. It is even more remarkable that it does so in a wild-type SNAP-25 background at the *Drosophila* larva NMJ. Although further analysis with expression of the mutant SNAP-25 in a null background is required to substantiate the present results, the consistency of the data reported here suggests that the presence of a single mutant SNARE complex in the very critical region of protein–protein contact between the petals of the rosette is sufficient to block the activity of the rosette. This does explain the dominant-negative nature of the mutation introduced here with respect to neuroexocytosis, and fits well with the specific action of BoNT/A and BoNT/C which cleave SNAP-25 just before and after Arg198, respectively, causing a dominant-negative effect with the characteristic long duration of action of these two neurotoxins (Eleopra et al., 1997; Eleopra et al., 1998; Meunier et al., 2003). The present model also explains the remarkable findings that the replacements of Lys201 and Leu203 with a negatively charged glutamate residue do not affect SNARE assembly but inhibits exocytosis in chromaffin cells (Criado et al., 1999; Gil et al., 2002) as these changes are disturbing the protein–protein contacts between adjacent SNARE complexes.

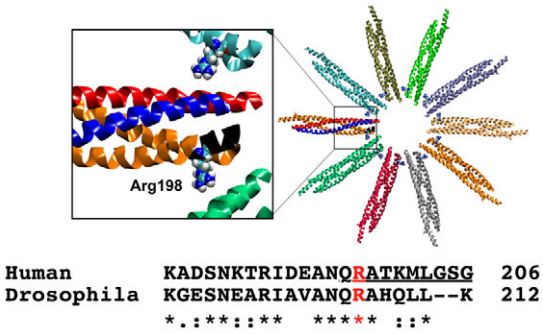

Fig. 7. Model of the SNARE complex rosette apparatus of neuroexocytosis. The number of SNARE complexes used here (ten) derives from an analysis of different experiments performed with botulinum neurotoxins type A and E on the frog neuromuscular junction (Raciborska et al., 1998) and on mouse spinal cord motoneurons (Keller and Neale, 2004). Clearly, the number ten is an approximate value, but it should be noted that using 8 to 13 complexes does not significantly change the position of the SNAP-25 Arg with respect to the neighbouring partner.

Materials and Methods

Plasmid generation and germline transformation in *Drosophila*

Two isoforms of SNAP-25 [SNAP-25^{R206A} and one wild-type SNAP-25^{WT}] were produced by PCR using primers carrying point mutations as necessary. The ORFs coding for SNAP-25 was amplified from the full-length cDNA derived

from w^{1118} flies using the following oligonucleotides: sense SNAP-25^{WT}, 5′-CGGAATTCATGCCAGCGGATCCATCTGAAG-3′; antisense SNAP-25^{WT}, 5′-CTCTCGAGTTACTTTAATAGTTGATGTGCC-3′; antisense SNAP-25^{R206A}, 5′-CTCTCGAGTTACTTTAATAGTTGATGTGCCgcTTGATTAGC-3′. Sense and antisense primers have at their 5′ ends the restriction sites for *Eco*RI and *Xho*I, respectively (underlined nucleotides). Mutated sites are in lower case letters.

After the initial denaturation step at 94°C for 3 minutes, amplification was achieved through 35 cycles at 94°C for 30 seconds, 55°C for 30 seconds, and 72°C for 2 minutes. A final extension reaction was carried out for 7 minutes at 72°C. The obtained 655 bp PCR products were ligated into the pCR2.1-TOPO vector (Invitrogen, USA) which was used to transform One Shot TOP10 *E. coli* cells. Positive clones were detected by β-galactosidase screening and sequencing (BRM Genomics, Italy). Using conventional restriction enzyme digestion techniques, sequences were extracted with *Eco*RI and *Xho*I and ligated into the pUAST *Drosophila* transformation vector.

The resulting plasmids, pUAS–SNAP-25^{WT} and pUAS–SNAP-25^{R206A} were again sequenced to ensure that the mutation occurred only at the position of interest and to verify the proper orientation inside the vector of each ORF (open reading frame). These plasmids were then used for embryo transformation.

P-element-mediated germline transformation was done using a *Drosophila* embryo injection service (Best Gene Inc, CA, USA). Briefly, the constructs with the w^{+} marker were injected into w^{1118} embryos. Nine independent transformant lines were established for each construct. *FM7* (X chromosome), *CyO* (chromosome 2) and *TM3(sb)* (chromosome 3) balancers were used to balance these lines.

Lines carrying the *UAS–SNAP-25^{WT}* transgene and the *UAS–SNAP-25^{R206A}* transgene were chosen on the basis of their homozygous viability. These new alleles of *SNAP-25* were expressed in flies with a *SNAP-25* wild-type background using the GAL4/UAS system. *ElavGAL4* virgin females were crossed to homozygous *UAS–SNAP-25^{WT}* and *UAS–SNAP-25^{R206A}* males.

Flies were raised on a standard yeast–glucose–agar medium and were maintained at 23°C, 70% relative humidity, in a 12 hour light:12 hour dark cycle. Experiments were carried out on F1 third instar larvae.

RNA extraction and semiquantitative PCR

Wild-type (WT) and mutant (R206A) *SNAP-25* mRNA expression levels were assessed in *ElavGAL4/UAS–SNAP-25^{WT}*, *ElavGAL4/UAS–SNAP-25^{R206A}* and control w^{1118} third instar larvae by semiquantitative PCR.

Total RNA was extracted from 12 brains (four for each line) of third instar larvae with TRIzol (Invitrogen, USA) following the manufacturer's instructions. RNA was treated with RQ1 RNAse-free DNAse (Promega, Italy) to avoid DNA contamination, and then resuspended in RNase-free water.

For each sample, 1 mg of RNA was used for the first-strand cDNA synthesis, employing oligonucleotides dT_{20} and SuperScript II (Invitrogen, USA) according to the manufacturer's instructions.

Semiquantitative PCRs were performed following the same PCR cycles described above. In each PCR reaction, a fragment of the constitutively expressed *rp49* mRNA and the 3′-term portion of one SNAP-25 isoform were amplified, using the following oligonucleotides: sense SNAP-25, 5′-GGATAACGAACGACGCTAGAGA-3′; antisense SNAP-25^{WT}, 5′-TACTTTAATAGTTGATGTGCCct-3′; antisense SNAP-25^{R206A}, 5′-CTTTAATAGTTGATGTGCCgc-3′; sense *rp49*, 5′-ATCGGTTACG-GATCGAACAA-3′; antisense *rp49*, 5′-GACAATCTCCTTGCGCTTCT-3′.

The size of the PCR products were 210 bp in the case of the SNAP-25 isoforms and 164 bp in the case of *rp49*. The samples were analysed by electrophoresis (1% agarose gel) and the resultant digital image of the gel was captured using a UV-transilluminator. The intensities of the bands were quantified using Image Pro Plus 6.0 (Media Cybernetics, USA). WT and R206A SNAP-25 isoform expression was calculated relative to the median values of the *rp49* housekeeping mRNA.

Site-directed mutagenesis

pGEX2T-SNAP-25^{WT} was used as template in a PCR amplification performed using the QuickChange site-directed mutagenesis kit (Stratagene). For the R198A mutation the forward primer was 5′-ATTGATGAAGCCAACCAAGCCGCAACAAA-GATGCTGGGAAGTGGT-3′. The mutated codon is underlined. PCR was performed under the following conditions: initial denaturation for 60 seconds at 95°C, amplification for 18 cycles of 50 seconds at 95°C, 50 seconds at 60°C and 11 minutes 30 seconds at 68°C, final extension for 7 minutes at 68°C. After digestion of the parental DNA for 1 hour at 37°C with *Dpn*I, the amplified plasmids were transformed into *E. coli* XL-1 Blue competent cells. The presence of the mutation was confirmed by DNA sequencing. The mutated construct was transformed into *E. coli* BL21 DE3 and the recombinant protein expressed.

Expression and purification of GST–SNAP-25 and GST–SNAP-25 mutants

SNAP-25^{WT} and its mutant R198A were expressed in *E. coli* BL21 DE3 as GST fusion proteins and isolated as previously described (Tonello et al., 1998). Briefly, expression of GST–SNAP-25^{WT} and GST–SNAP-25^{R198A} was induced for 3 hours at 30°C with 1 mM IPTG (isopropyl-β-D-thiogalactoside) and proteins were isolated on a glutathione–Sepharose 4B affinity column (Amersham Biosciences) according to the manufacturer's instructions. Resin-bound GST–SNAP-25^{WT} and GST–SNAP-25^{R198A} were eluted in a buffer containing 20 mM reduced glutathione and dialysed overnight in 10 mM Hepes buffer pH 7.4 with 150 mM NaCl. Protein purity was checked by SDS–PAGE on a 4–12% gel (Invitrogen).

Recombinant syntaxin 1A cytoplasmic domain (1–261) and VAMP2 cytoplasmic domain (1–96), a kind gift from B. Davletov (LMB, Cambridge, UK), were expressed and purified as described previously (Hu et al., 2002).

In vitro assembly of the SNARE complex

The reaction for assembly of the SNARE complex was performed as described previously (Fasshauer et al., 1998; Fasshauer et al., 2002; Hu et al., 2002). Recombinant VAMP2 and syntaxin 1A were incubated with either GST-SNAP-25^{WT} or the R198A mutant (30 pmol each) for different time periods at room temperature in 30 μl of 20 mM Hepes buffer pH 7.2, 150 mM NaCl, 1 mM Na_2EDTA, 1 mM dithiothreitol, 0.8% b-octyl glucoside. The reactions were stopped by the addition of sample loading buffer. The solutions were then incubated at room temperature or boiled at 100°C for 3 minutes (boiling disrupts the SNARE complex). Samples were then subjected to SDS-PAGE using NuPAGE 4–12% Precast gels (Invitrogen), followed by Coomassie Blue staining; images were collected with ChemiDoc^{TM} XRS (BioRad) and densitometric measurements were performed with WCIF ImageJ v1.35.

Electrophysiology

Experiments were performed at 20–22°C on third instar larval body wall preparations dissected in Ca^{2+}-free HL3 saline (Stewart et al., 1994) and pinned on the silicone-coated surface (Sylgard 184; Dow Corning, USA) of a 35 mm Petri dish (Bolatto et al., 2003). After dissection, Ca^{2+}-free HL3 saline was replaced with 1 mM Ca^{2+} HL3. Before starting electrophysiological recordings, third instar larval body walls were left to incubate in fresh 1 mM Ca^{2+} HL3 solution for at least 15 minutes.

Electrophysiological recordings were done on fibres 6 or 7 of abdominal segment 3 or 4 using intracellular glass microelectrodes (1.2 mm o.d.; 0.69 mm i.d.; 10–12 MΩ resistance; Science Products, Germany) filled with a 1:2 solution of 3 M KCl and 3 M CH_3CO_2K. Fibres with a membrane resting potential lower than –60 mV were discarded. In each fibre both spontaneous and evoked neurotransmitter release were recorded. No more than one fibre for each larval body wall was utilized for electrophysiological recording.

For quantifying Ca^{2+} dependence of both spontaneous and evoked neurotransmitter release, after dissection, body walls were first incubated in 1 mM Ca^{2+} for at least 15 minutes. After the spontaneous or evoked release was recorded, the bathing solution was replaced with one containing 3 mM Ca^{2+}, taking particular care to maintain in place the intracellular microelectrode and that resting membrane potential remained substantially unchanged (apart from the physiological shift due to the different extracellular Ca^{2+} concentrations). After an additional 15-minute incubation, spontaneous or evoked release was recorded again, and the bathing solution was changed to one containing 5 mM Ca^{2+}; following a further 15-minute incubation, a new recording of spontaneous or evoked release from the same fibre was performed. In all experiments, particular care was taken to avoid the microelectrode exiting from the fibre or fibre membrane damage; data from experiments in which this happened were discarded. Because evoked release can influence spontaneous neurotransmitter release, each activity was recorded in a separate set of experiments.

We did not observe any clear shift of resting membrane potential nor visible fibre alterations up to the end of the experiment (usually 60 minutes).

Intracellular recording of spontaneous neurotransmitter release

Spontaneous neurotransmitter release was analysed by intracellularly recording miniature end-plate potentials (MEPPs) under current clamp conditions. In a separate set of experiments miniature end plate currents (MEPCs) under voltage-clamp conditions were also recorded. This technique was used as it provides higher accuracy in the determination of spontaneous neurotransmitter release, and the possibility of using only one microelectrode for voltage-clamping because of the biophysical properties of the larval muscle fibre (Wu and Haugland, 1985). This particular advantage is lost when larger currents (for instance evoked excitatory junctional currents) must be clamped, making it necessary to use the more complex two-electrode voltage clamp (Wu and Haugland, 1985).

Signals were amplified by a patch-clamp amplifier (Axon 200A; Molecular Probe, USA) in current or voltage-clamp mode. When in voltage clamp mode, microelectrode series resistances were corrected to 95%. Resting membrane potential was clamped at –70 mV. Spontaneous release events were recorded for 240 seconds.

Intracellular recording of evoked neurotransmitter release

Evoked junction potentials (EJPs) were intracellularly recorded under current-clamp conditions. Resting membrane potential was clamped at –70 mV. The single segmental nerve innervating abdominal segment A3 or A4 was stimulated at 0.5 Hz (stimulus duration 0.1 milliseconds, 1.5 threshold voltage) using a suction microelectrode, filled with extracellular bathing solution and connected to a stimulator (S88, Grass, USA) via a stimulus isolation unit (SIU5, Grass, USA) in a capacitative coupling mode. Signals were amplified in current-clamp mode by a patch-clamp amplifier (Axopatch 200, Axon, USA).

Data analysis

Amplified signals were digitized using a digital A/C interface (National Instruments, USA) and then fed to a PC for both on-line visualisation and off-line analysis using an appropriate software (WinEDR, Starthclyde University; pClamp, Axon, USA). Stored data, were analysed off-line using appropriate software (pClamp, Axon, USA). Statistical analysis and graph construction were carried out using Prism software (GraphPad, USA).

Immunohistochemistry

NMJ synaptic boutons of A3–A4 fibres 6 and 7 were stained in body-wall preparations as previously described (Bolatto et al., 2003) using the presynaptic membrane marker anti-HRP antibody (1:300, Cappel MP Biomedicals, USA). Primary antibodies were detected with FITC-conjugated rabbit anti-goat IgG (1:300; Sigma-Aldrich, USA). Images were acquired with a video-confocal microscope (VCM; Mangoni Biomedica, Pisa, Italy) (Benedetti et al., 1995). Briefly, in VC microscopy an arc lamp is used as a multi-point excitation source and a CCD camera as an image detector. Confocal performance is achieved using an original processing method (Benedetti et al., 1995) (US patent 6.016.367), which allows high spatial resolution and spectral flexibility.

Optical sections of 0.5 μm were acquired using a ×20 0.75 NA dry objective. Acquired images were then collapsed into a single image with a maximum intensity projection algorithm. Bouton diameter was measured with NIS AR software (Nikon Instruments, Japan). Bouton area was measured on digital images, using ImageJ software. Statistical analysis of bouton areas and diameters was performed with Prism software.

Computational methods

Sequence conservation analysis was performed using the Bayesian method as implemented in the Consurf server (Landau et al., 2005). Molecular dynamic simulations were performed using, as a starting model, the SNARE structure (Chen et al., 2002), from which chain E, corresponding to the protein Complexin, was removed. Simulations were performed for the wild-type and Arg198Ala mutant using the generalized Born model approach for implicit solvation as implemented in AMBER software (Hawkins et al., 1996; Tsui and Case, 2000). A time step of 2 femtoseconds was adopted and the SHAKE algorithm (Ryckaert et al., 1977) was used to constrain chemical bonds. A cut off of 1.6 nm was adopted. Both wild-type and mutated systems were stabilized by 0.2 nanoseconds, during which the temperature was raised from 0 to 300 K coupling the systems to a Langevin thermostat with a collision frequency of 2/picosecond (Loncharich et al., 1992). Subsequently, 3 nanoseconds of production runs were performed for both systems.

We are grateful to B. Davletov for the kind gift of the sample of the recombinant cytoplasmic domain of VAMP/synaptobrevin and syntaxin. The present work was supported by Fondazione Cariparo Progetto “Physiopathology of the Synapse: Neurotransmitters, Neurotoxins and Novel Therapies” and Progetto Strategico of University of Padova: “An in vivo Approach to the Physiopathology of Signal Transduction”. M.S. was supported by a University of Padova grant (Assegno di Ricerca grant no. CPDR078721/07 and no. CPDR095880/09). D.Z. was supported by a Fondazione Cariparo grant. S.P. was supported by ANII (Agencia Nacional de Investigación e Innovación, Programa de Apoyo Sectorial a la Estrategia Nacional de Innovación) INNOVA URUGUAY (Agreement no. 8 DCI ALA/2007/19.040 between Uruguay and the European Commission).

Supplementary material available online at
http://jcs.biologists.org/cgi/content/full/123/19/3276/DC1

References

Antonin, W., Holroyd, C., Fasshauer, D., Pabst, S., Von Mollard, G. F. and Jahn, R. (2000). A SNARE complex mediating fusion of late endosomes defines conserved properties of SNARE structure and function. *EMBO J.* **19**, 6453-6464.

Benedetti, P. A., Evangelista, V., Guidarini, D. and Vestri, S. (1995). Electronic multiconfocal-points microscopy. *SPIE Proc.* **2412**.

Binz, T., Blasi, J., Yamasaki, S., Baumeister, A., Link, E., Sudhof, T. C., Jahn, R. and Niemann, H. (1994). Proteolysis of SNAP-25 by types E and A botulinal neurotoxins. *J. Biol. Chem.* **269**, 1617-1620.

Blasi, J., Chapman, E. R., Yamasaki, S., Binz, T., Niemann, H. and Jahn, R. (1993). Botulinum neurotoxin C1 blocks neurotransmitter release by means of cleaving HPC-1/syntaxin. *EMBO J.* **12**, 4821-4828.

Bolatto, C., Chifflet, S., Megighian, A. and Cantera, R. (2003). Synaptic activity modifies the levels of Dorsal and Cactus at the neuromuscular junction of Drosophila. *J. Neurobiol.* **54**, 525-536.

Brose, N. (2008). For better or for worse: complexins regulate SNARE function and vesicle fusion. *Traffic* **9**, 1403-1413.

Brunger, A. T., Weninger, K., Bowen, M. and Chu, S. (2009). Single-molecule studies of the neuronal SNARE fusion machinery. *Annu. Rev. Biochem.* **78**, 903-928.

Budnik, V. and Ruiz-Canada, C. (2006). The fly neuromuscular junction: structure and function. In *International Review of Neurobiology*, 2nd edn. San Diego: Academic Press.

Catterall, W. A. (1999). Interactions of presynaptic Ca^{2+} channels and snare proteins in neurotransmitter release. *Ann. NY Acad. Sci.* **868**, 144-159.

Chen, X., Tomchick, D. R., Kovrigin, E., Arac, D., Machius, M., Sudhof, T. C. and Rizo, J. (2002). Three-dimensional structure of the complexin/SNARE complex. *Neuron* **33**, 397-409.

Chernomordik, L. V. and Kozlov, M. M. (2008). Mechanics of membrane fusion. *Nat. Struct. Mol. Biol.* **15**, 675-683.

Cohen, F. S. and Melikyan, G. B. (2004). The energetics of membrane fusion from binding, through hemifusion, pore formation, and pore enlargement. *J. Membr. Biol.* **199**, 1-14.

Criado, M., Gil, A., Viniegra, S. and Gutierrez, L. M. (1999). A single amino acid near the C-terminus of the synaptosome-associated protein of 25 kDa (SANP-25) is essential for exocytosis in chromaffin cells. *Proc. Natl. Acad. Sci. USA* **96**, 7256-7261.

de Paiva, A., Ashton, A. C., Foran, P., Schiavo, G., Montecucco, C. and Dolly, J. O. (1993). Botulinum A like type B and tetanus toxins fulfils criteria for being a zinc-dependent protease. *J. Neurochem.* **61**, 2338-2341.

Eleopra, R., Tugnoli, V., Rossetto, O., Montecucco, C. and De Grandis, D. (1997). Botulinum neurotoxin serotype C: a novel effective botulinum toxin therapy in human. *Neurosci. Lett.* **224**, 91-94.

Eleopra, R., Tugnoli, V., Rossetto, O., De Grandis, D. and Montecucco, C. (1998). Different time courses of recovery after poisoning with botulinum neurotoxin serotypes A and E in humans. *Neurosci. Lett.* **256**, 135-138.

Fang, Q., Berberian, K., Gong, L. W., Hafez, I., Sorensen, J. B. and Lindau, M. (2008). The role of the C-terminus of the SNARE protein SNAP-25 in fusion pore opening and a model for fusion pore mechanics. *Proc. Natl. Acad. Sci. USA* **105**, 15388-15392.

Fasshauer, D., Eliason, W. K., Brunger, A. T. and Jahn, R. (1998). Identification of a minimal core of the synaptic SNARE complex sufficient for reversible assembly and disassembly. *Biochemistry* **37**, 10354-10362.

Fasshauer, D., Antonin, W., Subramaniam, V. and Jahn, R. (2002). SNARE assembly and disassembly exhibit a pronounced hysteresis. *Nat. Struct. Biol.* **9**, 144-150.

Gil, A., Gutierrez, L. M., Carrasco-Serrano, C., Alonso, M. T., Viniegra, S. and Criado, M. (2002). Modification in the C-terminus of the synaptosome-associated protein of 25 kDa (SNAP-25) and in the complementary region of synaptobrevin affect the final steps of exocytosis. *J. Biol. Chem.* **277**, 9904-9910.

Giraudo, C. G., Hu, C., You, D., Slovic, A. M., Mosharov, E. V., Sulzer, D., Melia, T. J. and Rothman, J. E. (2005). SNAREs can promote complete fusion and hemifusion as alternative outcomes. *J. Cell Biol.* **170**, 249-260.

Han, X., Wang, C. T., Bai, J., Chapman, E. R. and Jackson, M. B. (2004). Transmembrane segments of syntaxin line the fusion pore of Ca^{2+}-triggered exocytosis. *Science* **304**, 289-292.

Hawkins, G. D., Cramer, C. J. and Truhlar, D. G. (1996). Parametrized models of aqueous free energies of solvation based on pairwise descreening of solute atomic charges from a dielectric medium. *J. Phys. Chem.* **100**, 19824-19839.

Hu, K., Carroll, J., Rickman, C. and Davletov, B. (2002). Action of complexin on SNARE complex. *J. Biol. Chem* **277**, 41652-41656.

Hua, Y. and Scheller, R. H. (2001). Three SNARE complexes cooperate to mediate membrane fusion. *Proc. Natl. Acad. Sci. USA* **98**, 8065-8070.

Huang, X., Wheeler, M. B., Kang, Y. H., Sheu, L., Lukacs, G. L., Trimble, W. S. and Gaisano, H. Y. (1998). Truncated SNAP-25 (1-197), like botulinum neurotoxin A, can inhibit insulin secretion from HIT-T15 insulinoma cells. *Mol. Endocrinol.* **12**, 1060-1070.

Jahn, R. and Scheller, R. H. (2006). SNAREs-engines for membrane fusion. *Nat. Rev. Mol. Cell Biol.* **7**, 631-643.

Karatekin, E., Di Giovanni, J., Iborra, C., Coleman, J., O'Shaughnessy, B., Seagar, M. and Rothman, J. E. (2010). A fast, single-vesicle fusion assay mimics physiological SNARE requirements. *Proc. Natl. Acad. Sci. USA* **107**, 3517-3521.

Kasai, H. (1999). Comparative biology of Ca^{2+}-dependent exocytosis: implications of kinetic diversity for secretory function. *Trends Neurosci.* **22**, 88-93.

Keller, J. E. and Neale, E. A. (2001). The role of the synaptic protein snap-25 in the potency of botulinum neurotoxin type A. *J. Biol. Chem.* **276**, 13476-13482.

Keller, J. E., Cai, F. and Neale, E. A. (2004). Uptake of botulinum neurotoxin into cultured neurons. *Biochemistry* **43**, 526-532.

Landau, M., Mayrose, I., Rosenberg, Y., Glaser, F., Martz, E., Pupko, T. and Ben-Tal, N. (2005). ConSurf 2005, the projection of evolutionary conservation scores of residues on protein structures. *Nucleic Acids Res.* **33**, W299-W302.

Li, F., Pincet, F., Perez, E., Eng, W. S., Melia, T. J., Rothman, J. E. and Tareste, D. (2007). Energetics and dynamics of SNAREpin folding across lipid bilayers. *Nat. Struct. Mol. Biol.* **14**, 890-896.

Loncharich, R. J., Brooks, B. R. and Pastor, R. W. (1992). Langevin dynamics of peptides: the frictional dependence of isomerization rates of N-acetyl-alanyl-N′-methylamide. *Biopolymers* **32**, 523-535.

Lu, X., Zhang, Y. and Shin, Y. K. (2008). Supramolecular SNARE assembly precedes hemifusion in SNARE-mediated membrane fusion. *Nat. Struct. Mol. Biol.* **15**, 700-706.

Meunier, F. A., Lisk, G., Sesardic, D. and Dolly, J. O. (2003). Dynamics of motor nerve terminal remodeling unveiled using SNARE-cleaving botulinum toxins: the extent and duration are dictated by the sites of SNAP-25 truncation. *Mol. Cell. Neurosci.* **22**, 454-466.

Montecucco, C., Schiavo, G. and Pantano, S. (2005). SNARE complexes and neuroexocytosis: how many, how close? *Trends Biochem. Sci.* **30**, 367-372.

Neale, E. A., Bowers, L. M., Jia, M., Bateman, K. E. and Williamson, L. C. (1999). Botulinum neurotoxin A blocks synaptic vesicle exocytosis but not endocytosis at the nerve terminal. *J. Cell Biol.* **147**, 1249-1260.

Ohya, T., Miaczynska, M., Coskun, U., Lommer, B., Runge, A., Drechsel, D., Kalaidzidis, Y. and Zerial, M. (2009). Reconstitution of Rab- and SNARE-dependent membrane fusion by synthetic endosomes. *Nature* **459**, 1091-1097.

Pozzi, D., Condliffe, S., Bozzi, Y., Chikhladze, M., Grumelli, C., Proux-Gillardeaux, V., Takahashi, M., Franceschetti, S., Verderio, C. and Matteoli, M. (2008). Activity-dependent phosphorylation of Ser187 is required for SNAP-25-negative modulation of neuronal voltage-gated calcium channels. *Proc. Natl. Acad. Sci. USA* **105**, 323-328.

Raciborska, D. A., Trimble, W. S. and Charlton, M. P. (1998). Presynaptic protein interactions in vivo: evidence from botulinum A, C, D and E action at frog neuromuscular junction. *Eur. J. Neurosci.* **10**, 2617-2628.

Rickman, C., Hu, K., Carroll, J. and Davletov, B. (2005). Self-assembly of SNARE fusion proteins into star-shaped oligomers. *Biochem. J.* **388**, 75-79.

Rizo, J. and Rosenmund, C. (2008). Synaptic vesicle fusion. *Nat. Struct. Mol. Biol.* **15**, 665-674.

Rossetto, O., Caccin, P., Rigoni, M., Tonello, F., Bortoletto, N., Stevens, R. C. and Montecucco, C. (2001). Active-site mutagenesis of tetanus neurotoxin implicates TYR-375 and GLU-271 in metalloproteolytic activity. *Toxicon* **39**, 1151-1159.

Ryckaert, J., Ciccotti, G. and Berendsen, H. J. C. (1977). Numerical integration of the cartesian equations of motion of a system with constraints: molecular dynamics of n-alkanes. *J. Comput. Phys.* **23**, 327-341.

Schiavo, G., Benfenati, F., Poulain, B., Rossetto, O., Polverino de Laureto, P., DasGupta, B. R. and Montecucco, C. (1992). Tetanus and botulinum-B neurotoxins block neurotransmitter release by proteolytic cleavage of synaptobrevin. *Nature* **359**, 832-835.

Schiavo, G., Rossetto, O., Catsicas, S., Polverino de Laureto, P., Das Gupta, B. R., Benfenati, F. and Montecucco, C. (1993a). Identification of the nerve-terminal targets of botulinum neurotoxins serotypes A, D and E. *J. Biol. Chem.* **268**, 23784-23787.

Schiavo, G., Santucci, A., Dasgupta, B. R., Mehta, P. P., Jontes, J., Benfenati, F., Wilson, M. C. and Montecucco, C. (1993b). Botulinum neurotoxins serotypes A and E cleave SNAP-25 at distinct COOH-terminal peptide bonds. *FEBS Lett.* **335**, 99-103.

Sorensen, J. B. (2009). Conflicting views on the membrane fusion machinery and the fusion pore. *Annu. Rev. Cell Dev. Biol.* **25**, 513-537.

Sorensen, J. B., Wiederhold, K., Muller, E. M., Milosevic, I., Nagy, G., De Groot, B. L., Grubuller, H. and Fasshauer, D. (2006). Sequential N-to C-terminal SNARE complex assembly drives priming and fusion of secretory vesicles. *EMBO J.* **25**, 955-966.

Stewart, B. A., Atwood, H. L., Renger, J. J., Wang, J. and Wu, C. F. (1994). Improved stability of Drosophila larval neuromuscular preparations in haemolymph-like physiological solutions. *J. Comp. Physiol. A* **175**, 179-191.

Stewart, B. A., Mohtashami, M., Trimble, W. S. and Boulianne, G. L. (2000). SNARE proteins contribute to calcium cooperativity of synaptic transmission. *Proc. Natl. Acad. Sci. USA* **97**, 13955-13960.

Sudhof, T. C. and Malenka, R. C. (2008). Understanding synapses: past, present, and future. *Neuron* **60**, 469-476.

Sudhof, T. C. and Rothman, J. E. (2009). Membrane fusion: grappling with SNARE and SM proteins. *Science* **323**, 474-477.

Sutton, R. B., Fasshauer, D., Jahn, R. and Brunger, A. T. (1998). Crystal structure of a SNARE complex involved in synaptic exocytosis at 2.4 A resolution. *Nature* **395**, 347-353.

Tokumaru, H., Umayahara, K., Pellegrini, L. L., Ishizuka, T., Saisu, H., Betz, H., Augustine, G. J. and Abe, T. (2001). SNARE complex oligomerization by synaphin/complexin is essential for synaptic vesicle exocytosis. *Cell* **104**, 421-432.

Tonello, C., Dioni, L., Briscini, L., Nisoli, E. and Carruba, M. O. (1998). SR59230A blocks beta3-adrenoceptor-linked modulation of upcoupling protein-1 and leptin in rat brown adipocytes. *Eur. J. Pharmacol.* **352**, 125-129.

Tsui, V. and Case, D. A. (2000). Theory and applications of the generalized Born solvation model in macromolecular simulations. *Biopolymers* **56**, 275-291.

Wei, S., Xu, T., Ashery, U., Kollewe, A., Matti, U., Antonin, W., Rettig, J. and Neher, E. (2000). Exocytotic mechanism studied by truncated and 0 layer mutants of the C-terminus of SNAP-25. *EMBO J.* **19**, 1279-1289.

Wu, C. F. and Haugland, F. N. (1985). Voltage clamp analysis of membrane currents in larval muscle fibers of Drosophila: alteration of potassium currents in Shaker mutants. *J. Neurosci.* **5**, 2626-2640.

Yersin, A., Hirling, H., Steiner, P., Magnin, S., Regazzi, R., Huni, B., Huguenot, P., De los Rios, P., Dietler, G., Catsicas, S. et al. (2003). Interactions between synaptic vesicle fusion proteins explored by atomic force microscopy. *Proc. Natl. Acad. Sci. USA* **100**, 8736-8741.

Zenisek, D., Steyer, J. A. and Almers, W. (2000). Transport, capture and exocytosis of single synaptic vesicles at active zones. *Nature* **406**, 849-854.

Zhong, H., Yokoyama, C. T., Scheuer, T. and Catterall, W. A. (1999). Reciprocal regulation of P/Q-type Ca2+ channels by SNAP-25, syntaxin and synaptotagmin. *Nat. Neurosci.* **2**, 939-941.